Photoelectron spectroscopy of deprotonated benzonitrile

Eleanor K. Ashworth[1] and James N. Bull[1, 2, a)]
[1)] *School of Chemistry, Norwich Research Park, University of East Anglia, Norwich NR4 7TJ, United Kingdom*
[2)] *Centre for Photonics and Quantum Science, University of East Anglia, Norwich NR4 7TJ, United Kingdom*

The recent discovery of cyano-substituted aromatic and two-ring PAH molecules in Taurus Molecular Cloud-1 have prompted questions on how the electronic structure and excited-state dynamics of these molecules are linked with their existence and abundance. Here, we report a photodetachment, and frequency- and angle-resolved photoelectron spectroscopy study of jet-cooled *para*-deprotonated benzonitrile (*p*-[Bzn–H]$^-$). The adiabatic detachment energy (ADE) was determined as 1.70±0.01 eV, in good agreement with CCSD(T)/aug-cc-pVTZ calculations. The spectra across the first few electronvolts above threshold are dominated by prompt autodetachment processes associated with excitation of at least five short-lived (tens of femtoseconds) temporary anion shape resonances since excitation cross-sections are several orders of magnitude larger than direct photodetachment cross-sections. The photoexcitation vibronic profile is dominated by a ≈640 cm^{-1} ring deformation mode. [Bzn–H]$^-$ lacks a valence-localized excited state situated below the detachment threshold and does not exhibit thermionic emission following excitation of the temporary anion resonances. Thus, [Bzn–H]$^-$ is unlikely to be stable in many interstellar environments.

I. INTRODUCTION

Carbonaceous astrochemistry has become a topical field over the last few decades due to the widespread infrared fingerprints, and related phenomena, observed to originate from carbon-based molecules in space.[1,2] In particular, the interest in astrochemical aromatic and polycyclic aromatic hydrocarbon (PAH) molecules has been spurred by the assignment of several diffuse interstellar bands (DIBs) to C_{60}^+,[3] and the identification of several two-ring PAHs.[4–7] The preponderance of aromatic carbon molecules, most likely as large PAHs as a general class, in space is being further highlighted by the deployment of the James Webb Space Telescope, providing widespread observations of infrared bands linked with their vibrational emissions.[8] In addition to these larger PAHs, smaller substituted, aromatic molecules have also been identified in the Taurus Molecular Cloud-1 (TMC-1), including benzonitrile and cyanocyclopentadiene.[4,9] These small aromatics are considered as the fundamental building blocks in 'bottom-up' growth models for larger PAH molecules,[10,11] where growth occurs through neutral-neutral, ion-neutral, and cation-anion neutralization reactions followed by radiative cooling to stabilize the product.

Benzonitrile (Bzn, FIG. 1) is an appealing target for laboratory studies because it is the smallest heteroaromatic molecule known to exist in space and it is readily introduced into gas-phase experiments due to its' volatility (melting point $T \approx 260$ K). Consequently, there have been several studies on the dissociation processes of cationic[14,15] and protonated[16] Bzn, which are likely positive charge carriers in astrochemical environments where benzonitrile is present. Most laboratory-based studies on potential interstellar aromatic ions have focussed on cations, due to the the greater propensity for cation presence in the interstellar medium (ISM), the enhanced applicability of ion sources to cation formation, and the capabilities of mass spectrometry laboratory instrumentation to isolate and probe cation photodissociation dynamics. Nevertheless, considering that some 20% of carbon in the ISM is assumed to be tied up as PAHs,[17,18] and also that anions are often considered as the main source of negative charge in space,[19] it is important to understand the electronic structure and excited-state dynamics of aromatic molecular anions that could exist in the ISM.[20] For Bzn, a combined photoelectron spectroscopy and computational study on the radical anion identified a low detachment energy (≈0.1 eV),[12,13] which implies that the anion is unlikely to exist in space. However, CN^-, the likely dissociation product from Bzn^- has been observed in TMC-1,[21] as have the linear carbon anions $C_{2n+1}N^-$

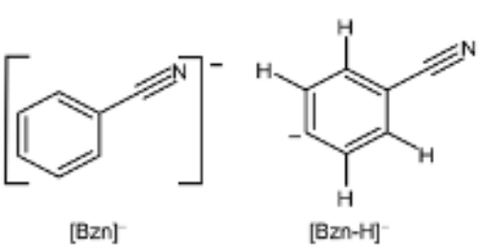

FIG. 1. Structures of anionic benzonitrile, [Bzn]$^-$ and *para*-deprotonated benzonitrile [Bzn-H]$^-$. [Bzn]$^-$ has a very low electron detachment energy (≈0.058 eV),[12,13] and is consequently unlikely to exist in space. The *ortho*- and *meta*-structural isomers of [Bzn-H]$^-$ are shown in FIG. S1 in the Supplementary Material.

[a)] Electronic mail: james.bull@uea.ac.uk

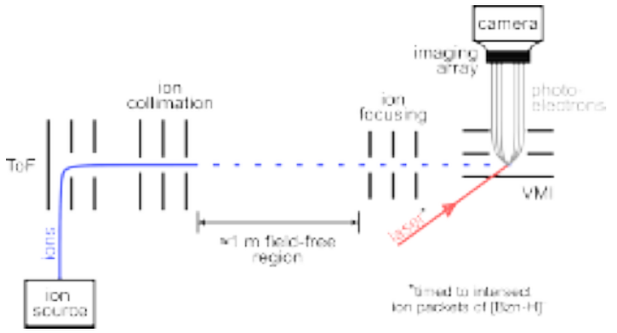

FIG. 2. Schematic diagram of the photodetachment-photoelectron instrument. Ion trajectories follow the blue trace. Complete instrument details are given in Ref. 28. The time-of-flight path length is ≈1 m, providing a resolving power of $\frac{m}{\Delta m} \approx 600$. The VMI was operated with a repeller voltage of $V_{rep} = -500$ V and an extractor voltage of $0.72 \times V_{rep}$.

($n = 2, 3$) and $C_{2n}H^-$ ($n = 1 - 5$),[21–27] which possess a closed-shell electronic structure, suggesting that [Bzn-H]$^-$ (FIG. 1), with a similar electronic structure, is a likely interstellar candidate.

Here, we report a photodetachment (PD) and photoelectron (PE) spectroscopy study using velocity-map imaging over the ≈13500–32000 cm^{-1} range on [Bzn–H]$^-$, produced in a jet-cooled plasma discharge source. We demonstrate that electron detachment is dominated by prompt autodetachment processes following resonant excitation of at least five temporary negative anion (shape) resonances.

II. METHODS

A. Experimental

The photodetachment spectrum and photoelectron velocity-map images were recorded using a custom-built instrument (FIG. 2), which is described in detail in Ref. 28. For the present measurements, a gas mixture of ≈1% benzonitrile (from a liquid sample, ThermoFisher >99%) in N_2 (total backing pressure ≈2 bar) was used as the feedstock. This gas mixture was introduced into plasma source (pair of needles of <1 mm diameter, <1 mm separation in a PEEK block) using a Parker series 9 pulsed valve (260 μs opening duration).[28] Anions formed in the plasma undergo supersonic expansion and jet cooling on exiting the plasma source, reaching a vibrational temperature of $T \leq 50$ K. The nascent anions were separated according to their m/z ratio by a Wiley-McLaren time-of-flight (ToF) mass spectrometry region, and were quantified using a Photonis BiPolar ToF detector. The experiment was operated at 20 Hz, as defined by the maximum repetition rate of the laser system.

The photodetachment signal and photoelectron velocity-map images were recorded by focussing the anions through the center of a velocity-map imaging electrode stack (≈10^{-8} mbar). Light pulses from an EKSPLA NT342 OPO (optical parametric oscillator) laser were timed to interact with the m/z of interest (m/z=102 for [Bzn-H]$^-$). Light fluence was typically 2–3 mJ pulse^{-1} and loosely focussed to a circle of ≈2.5 mm diameter. These conditions were chosen to minimize any multiphoton absorption processes. Velocity-mapped photoelectrons were imaged using a Photek VID240 detector, consisting of dual 40 mm diameter microchannel plates (MCPs) coupled with a P43 phosphor screen. The second MCP was connected to a gating unit, which minimized ion and laser background. The phosphor was monitored using a triggered Blackfly S (monochrome, Sony IMX252 CMOS) camera with a 6 mm focal length lens. Typical velocity-map images were recorded over 500–15000 laser shots (depending on photoelectron signal level). Velocity-map images were reconstructed using a polar onion peeling algorithm,[29] and the velocity to kinetic energy conversion was calibrated using the atomic line spectrum from photodetachment of I$^-$.

B. Electronic structure calculations

In principle, [Bzn–H]$^-$ could be generated as three structural isomers: *ortho*, *meta*, and *para* see illustrations in the Supplementary Material (FIG. S1). Equilibrium geometries of *o*-, *m*-, and *p*-[Bzn–H]$^-$ were optimized at the MP2/aug-cc-pVTZ level of theory (with zero-point energy correction), followed by CCSD(T) single-point energy calculations.[30–36]

Temporary anion resonances (vertical transition energies and oscillator strengths) were calculated using the CAP-EOM-EA-CCSD/aug-cc-pVDZ and CAP-EOM-CCSD/aug-cc-pVDZ levels of theory,[37–39] as implemented in Q-Chem 6.1,[40] using the (cuboid) CAP parameters CAPETA=1000, CAP X=1800, CAP Y=1500, and CAPY Z=1500. Photoelectron angular distributions (PADs) for direct photodetachment, which were quantified as β_2 parameters,[41] were simulated using the Q-Chem/ezDyson protocol with the CAP-EOM-IP-CCSD/aug-cc-pVDZ level of theory. Dyson orbitals were computed using Q-Chem 6.1,[40] and the resulting output used for ezDyson 5[42] calculations (translated in energy using the CCSD(T)/aug-cc-pVTZ ionization energy). The $D_1 \leftarrow D_0$ vertical excitation energy was computed at the EOM-CCSD/aug-cc-pVDZ level of theory.[37] Electronic excitation spectral profiles were modelled at the ωB97X-D/aug-cc-pVTZ level of theory using the Franck-Condon-Herzberg-Teller framework as implemented in Gaussian 16.[43]

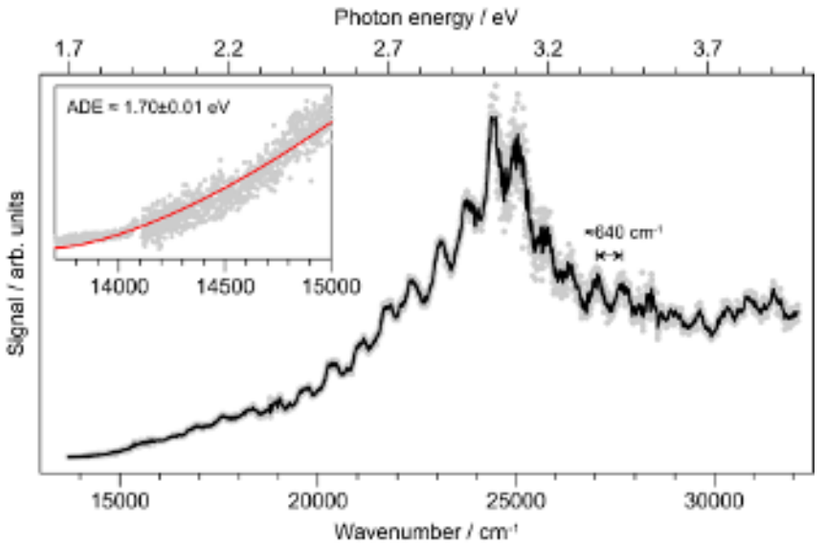

FIG. 3. Photodetachment spectrum for $[Bzn–H]^-$ (grey points) with a seven-point running average (black line). The apparent vibrational structure corresponds to a frequency of $\nu \approx 640\,\mathrm{cm}^{-1}$. Inset is the threshold region from 13700–15000 cm^{-1}, with the Wigner threshold law fit curve in red (ADE = 1.70±0.01 eV). The simulated $D_0 \leftarrow S_0$ direct photdetachment spectrum is shown in the Supplementary Material (FIG. S3), and spans ≈0.5 eV. As discussed in the text, the direct photodetachment cross-section is small compared with photoexcitation of temporary anion resonances.)

III. RESULTS AND DISCUSSION

A. Photodetachment spectrum

The photodetachment spectrum recorded for $[Bzn–H]^-$ over the 13699–32116 cm^{-1} range is shown in FIG. 3. The spectrum features a steady rise from the threshold region (13699–15000 cm^{-1}) to the main peak (≈24400 cm^{-1}). The main body of the spectrum exhibits a series of peaks with ≈640 cm^{-1} spacing, with a ≈360 cm^{-1} full-width half-maximum (corresponding to a 14±2 fs lifetime).

We assign the photodetachment spectrum to the *p*-$[Bzn–H]^-$ isomer based on a fit of the threshold region (FIG. 3, inset) to the Wigner threshold law,[44] providing the adiabatic detachment energy (ADE) at 1.70±0.01 eV. This value is in good agreement with the ADE computed at the CCSD(T)/aug-cc-pVTZ level of theory (1.83 eV) for *para* isomer. The *meta* and *ortho* isomers have calculated ADE values at 1.95 eV and 2.10 eV, respectively. We note density functional theory calculations by Firth et al.[45] also predicted the *para* isomer to have the lowest ADE. Our assignment to the *para* isomer is further supported through calculations of the relative energies of the isomers, which found that the *meta* and *ortho* isomers lie much higher in energy, relative to the *para* isomer, at 1.92 eV and 1.82 eV, respectively. Because the ions are generated in a hot plasma source and survive for some microseconds before being cooled through a supersonic expansion, they have ample time to undergo rearrangement to the most stable thermodynamic isomer. The calculated vertical detachment energy for the *para* isomer is 2.08 eV, however, as we will describe, this parameter is difficult to assign experimentally because autodetachment is a far more dominant process than direct photodetachment.

It is worth noting that neutral molecules possessing a permanent electric dipole moment of $|\mu| > 1.625$ D (theoretical value) support a dipole-bound state (DBS),[46,47] although, in practise, a value of $|\mu| > 2.5$ D is necessary due to centrifugal effects.[48] Calculated values of $|\mu|$ for [Bzn–H] are $|\mu| = 3.99$ D (neutral optimized geometry) and $\mu = 3.86$ D (anion optimized geometry), consistent with a DBS with a binding energy of 50–60 meV. However, because the DBS is situated below the detachment threshold and apparently shows little vibrational structure (i.e. no band progression over the near-threshold region), we do not observe any DBS signatures in our single-color experiments. Furthermore, the simulated direct photodetachment spectrum for $[Bzn–H]^-$ (FIG. S3 in the Supplementary Material) is extended (spanning ≈0.5 eV), similar to the phenide anion studied with photoelectron spectroscopy by Lineberger and co-workers,[49] with a direct photodetachment spectrum that spans nearly 1 eV. Consequently, the vibrational progression associated with DBS excitation and autodetachment, if observable, should involve many weak features over first 0.5 eV above-threshold. This conclusion is consistent with the fact that vertical excitation cross-sections to all DBS transitions in related nitrogen-containing aromatic anions (with similar valance electron binding energies) are orders of magnitude lower than to the shape

resonances.[50]

To aid in interpretation of the photodetachment spectrum, we computed the excited electronic states of $[Bzn–H]^-$ (FIG. 4) using the CAP-EOM-CCSD/aug-cc-pVDZ methodology. For photon energies within our window of study, seven excited states are accessible, although one (S_4) has zero oscillator strength. The others have vertical excitation cross-sections of S_1 – 8.5×10^2 Å^2, S_2 – 2.4×10^3 Å^2, S_3 – 2.4×10^2 Å^2, S_5 – 1.2×10^4 Å^2, S_6 – 1.4×10^3 Å^2, and S_7 – 1.0×10^3 Å^2. The transition energy of the brightest state (S_5) calculated at 3.01 eV, is consistent with the maximum of the photodetachment spectrum. These excited states are all classed as temporary anion shape resonances because they lie within the detachment continuum and involve HOMO $\rightarrow \pi^*/\sigma^*$ transitions. An EOM-CCSD calculation on the radical neutral indicates that the D_1 state lies 3.8 eV above the D_0 state, leading to the conclusion that $D_0 \leftarrow S_0$ is the only direct photodetachment that contributes to most of our spectrum. The simulated direct photodetachment cross-section spans 0.13 Å^2 at $h\nu = 2.18$ eV to 0.30 Å^2 at $h\nu = 3.93$ eV (maximum value across the simulated range), which are several orders of magnitude lower than those for excitation. We conclude that our photodetachment spectrum is dominated by autodetachment and that direct photodetachment makes only a minor contribution. Additional evidence for this conclusion is given in the next section through comparison of experimental and simulated photoelectron anisotropy distributions.

We now consider the vibrational structure evident in the photodetachment spectrum, which appears to have ≈640 cm^{-1} spacing. Because the spectrum is dominated by autodetachment after photoexcitation, we performed Franck-Condon-Herzberg-Teller simulations of the absorption profiles (see Supplementary Material). The autodetachment processes occur *via* (at least) seven overlapping shape resonances (FIG. S3). A common feature of all of the excitation profiles is activity of a ring deformation mode (as the fundamental and as part of combination bands) with a harmonic frequency of ≈650 cm^{-1} (see illustration in FIG. S2; the frequency varies slightly for each excited state). Although there are several overlapping electronic states, if we take the full-width half-maximum of two most prominent vibrational features (at ≈3.0 and ≈3.1 eV), which likely corresponds vertical excitation of the brightest excited state (S_5), we obtain a 14±2 fs lifetime, which is consistent with the expected lifetime from a shape resonance.[51,52]

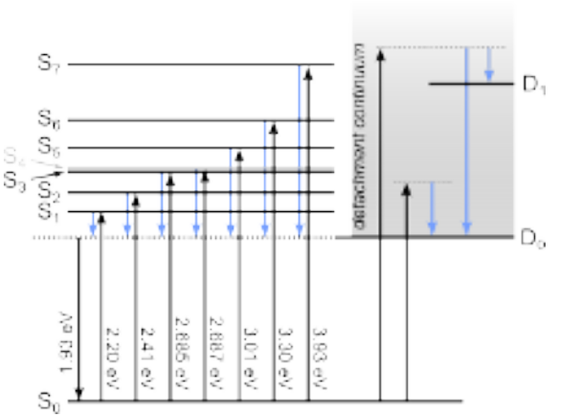

FIG. 4. Schematic energy level diagram for $[Bzn–H]^-$. Prompt autodetachment occurs *via* excitation to one of the seven excited states accessible over the photon energy range of the experimental data (1.8–4.0 eV). The S_n excited states, which are formally all shape resonances because they are situated in the detachment continuum and involve HOMO $\rightarrow \pi^*/\sigma^*$ excitations, were computed at the CAP-EOM-EA-CCSD/aug-cc-pVDZ level of theory. The D_1 excitation energy (≈3.8 eV) was computed at the EOM-CCSD/aug-cc-pVDZ. The S_4 state is greyed as it has zero oscillator strength. The S_5 state [$(2)^1A_1$] has the largest excitation cross-section at 1.2×10^4 Å^2. Black arrows indicate excitation energies, and blue arrows show direct photodetachment electron kinetic energies. It should be noted that, although the structure of $[Bzn–H]^-$ might appear close to that of deprotonated benzene (phenide, $C_6H_5^-$),[49] the addition of the cyanide group substantially changes the energy level structure of the anion (see FIG. S4 for phenide energy levels).

B. Photoelectron spectra and PADs

The 2D photoelectron spectrum or map, shown in FIG. 5a, was constructed from 130 individual photoelectron spectra spanning the $h\nu = 1.75$–4.00 eV photon energy range. The photodetachment spectrum is shown in FIG. 5b to allow for correlation of spectral features, while selected photoelectron spectra are shown in FIG. 5c–e. Over the $h\nu < 3.1$ eV range, the 2D map shows a systematic oscillation between high-eKE electrons coincident with dips in the photodetachment spectrum and a broadened distribution extended to lower-eKE coincident with peaks in the photodetachment spectrum (e.g. compare the two spectra shown in FIG. 5d). These spectra also have differing β_2 angular anisotropies, indicative of ejection processes from different electronic states. This oscillation is consistent with the ≈640 cm^{-1} peak spacing in the PD spectrum (assigned to ring deformation). This corresponds to the ≈650 cm^{-1} ring deformation mode of *p*-$[Bzn–H]^-$ identified in Franck-Condon-Herzberg-Teller simulations (the corresponding mode in the highly-unstable *ortho* isomer is calculated at 632 cm^{-1}, and 571 cm^{-1} for the *meta* isomer, clearly discounting the latter). We note that each of the recorded photoelectron spectra exhibit some (unresolved) vibrational structure, indicating that autodetachment occurs to at least two vibrational levels of the neutral.

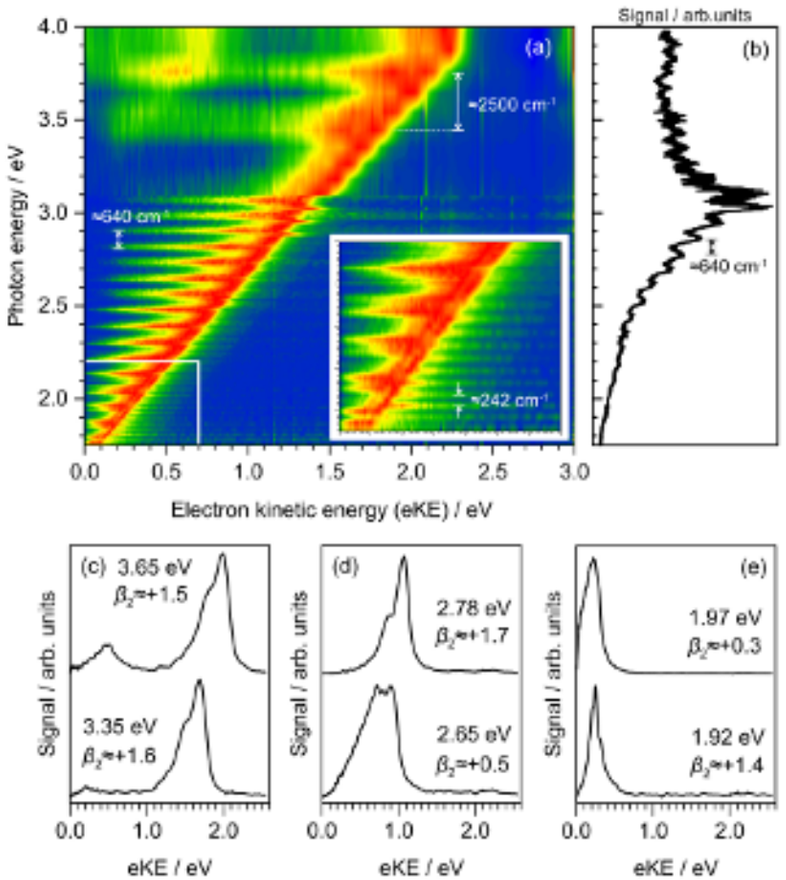

FIG. 5. Photodetachment-photoelectron spectroscopy of $[\text{Bzn–H}]^-$: (a) 2D spectrum or map over the $h\nu = 1.75$–$4.00\,\text{eV}$ (14115–$32262\,\text{cm}^{-1}$) photon energy range. Each photoelectron spectrum was normalized to have unit maximum signal intensity. Inset is an expansion of the low photon energy region ($h\nu < 2.2\,\text{eV}$). (b) Photodetachment spectrum (seven-point running average) over the same range as in FIG. 3. (c)–(e) Selected photoelectron spectra (seven-point running average), at given photon energies and with corresponding β_2 values (±0.1), from regions (c) $h\nu > 3.1\,\text{eV}$, (d) $h\nu = 3.1$–$2.2\,\text{eV}$, and (e) $h\nu < 2.2\,\text{eV}$. See the Supplementary Material for β_2 value plots.

A second vibrational feature is evident for $h\nu < 2.1\,\text{eV}$ over which the spectrum is dominated by direct photodetachment (the $S_1 \leftarrow S_0$ vertical transition is calculated at 2.20 eV). This region is shown expanded in the inset in FIG. 5a and features an oscillation with spacing of $\approx 242\,\text{cm}^{-1}$, consistent with a progression of vibrations involving CN wagging modes and associated combination bands. From the example spectrum in FIG. 5e, we obtain the ADE of $1.67 \pm 0.05\,\text{eV}$, consistent with the value from the photodetachment spectrum. Because the direct photodetachment feature is swamped by prompt autodetachment in higher photon energy photoelectron spectra, we cannot reliably extract electron detachment energies from these spectra.

For photon energies $h\nu > 3.3\,\text{eV}$, new low-eKE features appear in the spectrum (see example spectra in FIG. 5c) with an apparent photon energy spacing of $\approx 2500\,\text{cm}^{-1}$, consistent with the CN stretching mode of $[\text{Bzn–H}]^-$ (see illustration in the Supplementary Material). The appearance of this new feature is consistent with the emergence of the $D_1 \leftarrow S_0$ direct photodetachment channel.

An advantage of velocity-map imaging is the simultaneous determination of PADs, quantified in terms of a β_2 anisotropy parameters (FIG. S5). Briefly, the β_2 values reflect the symmetries of orbitals from which the electron was ejected convoluted with the timescale over which the electron was ejected – for $\beta_2 = -1$ electron ejection occurs perpendicular to the laser polarization axis, while for $\beta_2 = +2$, ejection occurs parallel to the laser polarization axis.[41] While our photoelectron velocity-map images show some β_2 trends, e.g. from FIG. 5d, photon energies resonant with peaks in the photodetachment spectra ($h\nu = 2.2$–$3.1\,\text{eV}$) produced narrower and highly anisotropic eKE distributions ($\beta_2 = +1.6 \pm 0.1$), and non-resonant photon

energies produced an extended eKE distribution with less anisotropy ($\beta_2 = +0.5 \pm 0.1$), the number of overlapping excited states means a quantitative interpretation is not possible. However, we can make two broad statements: (i) because an anisotropic β_2 indicates that electron ejection occurs faster than molecular rotation ($\approx$1 ps for [Bzn-H]$^-$), the electron detachment processes are prompt and no long-lived states are involved; (ii) modeling of the anisotropies for $D_1 \leftarrow S_0$ direct photodetachment process (FIG. S6) indicated negative β_2 values for photon energies over our spectra range, which is inconsistent with observation of positive β_2 values in the experimental data. Point (ii) supports that direct photodetachment is a minor process compared with excitation followed by prompt autodetachment.

We found no evidence for thermionic emission in the photoelecton spectra, which is an electron detachment process that occurs following internal conversion to the ground electronic state and, in turn, statistical electron ejection over a nanosecond to microsecond timescale.[53] Such processes are characterised by an isotropic, low-eKE Boltzmann-like distributions in the photoelectron spectra,[54] and through delaying of the gating unit on the MCP detector (as to gate out any electron detachment signal occurring faster than a few nanoseconds).[55] The lack of any thermionic emission signal implies that no excited state resonance accessed over our photon energy range survives long enough for internal conversion to occur, recovering the ground electronic state.

C. Astrochemical considerations

Stable molecular anions in space are thought to form through two mechanisms:[20] (i) radiative electron attachment, whereby a free electron is captured by a temporary anion resonance or DBS,[56] followed by internal conversion to ground electronic state and liberation of energy through radiative cooling (IR emission and recurrent fluorescence),[57,58] or (ii) dissociatve electron attachment, whereby a large molecular anion captures an electron which causes bond cleavage to give a smaller stable anion and neutral.[59] Astronomical observations on anion:neutral column densities for the known $C_{2n}H^-$ and $C_{2n+1}N^-$ species, and modelling of rate coefficients, have largely concluded that process (i) is the most probable.[60,61] In efforts to understand the radiative cooling dynamics of small carbonaceous cations, work using the DESIREE infrastructure,[62] including by the current authors,[63–66] has sought to characterize the rates for radiative emission, finding that infrared emission and, critically, recurrent fluorescence (emission from thermally populated electronic states) are important for efficient radiative stabilization.[67] Furthermore, as detailed in the introduction, a key requirement for a stable interstellar anion is a high electron affinity and, presumably, some degree of resilience to the interstellar radiation field towards photodetachment.[57,68] For context, the $C_{2n}H^-$ and $C_{2n+1}N^-$ species that exist in TMC-1 are all closed-shell species that support a DBS (C_2H^- does not support a DBS and has not been observed in the ISM) and have electron affinities >3.6 eV.[69,70] Most of these anions (except C_4H^- and CN^-) have valence-localized excited states situated below the detachment threshold that would be required for recurrent fluorescence radiative cooling.[71,72]

Ultimately, we conclude that while benzonitrile has been identified in the ISM,[4] [Bzn–H]$^-$ is unlikely to be stable under interstellar conditions involving any UV radiation field (e.g. photodissociation region) due to its lower electron affinity (1.70 eV) and high density of just-above-threshold excited states, which have substantial excitation cross-sections that lead to autodetachment rather than internal conversion to recover the ground electronic state (i.e. there is no evidence for thermionic emission). Examples of anions whose properties are conducive to recurrent fluorescence (i.e. those that exhibit thermionic emission following above-threshold excitation detected and have a suitable energy level structure) include C_{60}^-[73,74] and the menadione radical anion.[53] In the case of [Bzn–H]$^-$, there is no evidence of thermionic emission in the photoelectron data (FIG. 5a), and there are no bound, valence-localized anion excited states. This implies that [Bzn–H]$^-$ is unlikely to be stable under interstellar conditions, as it does not exhibit the experimental signatures or properties expected of a molecule compatible with interstellar environments. Ideally, future efforts might like to systematically study the cooling and stabilization dynamics of the known interstellar anions in order to help establish predictive rules of thumb for their interstellar existence and abundance.

IV. CONCLUSIONS

Photodetachment and photoelectron spectra of jet-cooled *p*-[Bzn–H]$^-$ have been reported, providing the adiabatic electron affinity of 1.70±0.01 eV, and demonstrating that the action spectra over the first few electron-volts above threshold are dominated by autodetachment from temporary anion states (shape resonances). There is no evidence for internal conversion to the ground electronic state. The lower electron affinity combined with the lack of internal conversion dynamics implies that *para*-[Bzn–H]$^-$ will not be a stable interstellar anion in environments where there is a UV radiation field. The fact that a large fraction of carbon in space exists as aromatic molecules implies that rigorously characterizing the electron-molecule interactions of such aromatics is important for establishing the fundamental data and trends required to predict interstellar anion abundance. Future studies, which may use the present methodology, should consider small aromatic anions with electron affinities closer to or above 3.6 eV. This may

include two- and three-ring deprotonated cyano-PAHs.

SUPPLEMENTARY MATERIAL

The Supplementary Material contains details on: important vibrational modes of p-[Bzn–H]$^-$, simulated Franck-Condon-Herzberg-Teller photoexcitation spectra and the direct photodetachment spectrum, energy level diagram for phenide, summary of experimental and simulated β_2 values, optimized geometries of [Bzn–H]$^-$ isomers.

DATA AVAILABILITY

All experimental and calculated data as part of this study are available from the authors upon reasonable request.

ACKNOWLEDGMENTS

Funding was provided by an EPSRC New Investigator Award (EP/W018691 to JNB). EKA thanks the University of East Anglia for doctoral studentship. Electronic structure calculations were, in part, carried out on the High Performance Computing Cluster supported by the Research and Specialist Computing Support service at the University of East Anglia.

CONFLICTS OF INTEREST

The authors have no conflicts to disclose.

REFERENCES

[1]P. Ehrenfreund and S. B. Charnley, Ann. Rev. Astronom. Astrophys. **38**, 427 (2000).
[2]E. Herbst and E. F. van Dishoeck, Ann. Rev. Astronom. Astrophys. **47**, 427 (2009).
[3]E. K. Campbell, M. Holz, D. Gerlich, and J. P. Maier, Nature **523**, 322 (2015).
[4]B. A. McGuire, A. M. Burkhardt, S. Kalenskii, C. N. Shingledecker, A. J. Remijan, E. Herbst, and M. C. McCarthy, Science **359**, 202 (2018).
[5]B. A. McGuire, R. A. Loomis, A. M. Burkhardt, K. L. K. Lee, C. N. Shingledecker, S. B. Charnley, I. R. Cooke, M. A. Cordiner, E. Herbst, S. Kalenskii, M. A. Siebert, E. R. Willis, C. Xue, A. J. Remijan, and M. C. McCarthy, Science **371**, 1265 (2021).
[6]A. M. Burkhardt, K. Long Kelvin Lee, P. Bryan Changala, C. N. Shingledecker, I. R. Cooke, R. A. Loomis, H. Wei, S. B. Charnley, E. Herbst, M. C. McCarthy, and B. A. McGuire, The Astrophysical Journal Letters **913**, L18 (2021).
[7]M. L. Sita, P. B. Changala, C. Xue, A. M. Burkhardt, C. N. Shingledecker, K. L. Kelvin Lee, R. A. Loomis, E. Momjian, M. A. Siebert, D. Gupta, E. Herbst, A. J. Remijan, M. C. McCarthy, I. R. Cooke, and B. A. McGuire, The Astrophysical Journal Letters **938**, L12 (2022).
[8]J. S. Spilker, K. A. Phadke, M. Aravena, M. Archipley, M. B. Bayliss, J. E. Birkin, M. Béthermin, J. Burgoyne, J. Cathey, S. C. Chapman, H. Dahle, A. H. Gonzalez, G. Gururajan, C. C. Hayward, Y. D. Hezaveh, R. Hill, T. A. Hutchison, K. J. Kim, S. Kim, D. Law, R. Legin, M. A. Malkan, D. P. Marrone, E. J. Murphy, D. Narayanan, A. Navarre, G. M. Olivier, J. A. Rich, J. R. Rigby, C. Reuter, J. E. Rhoads, K. Sharon, J. D. T. Smith, M. Solimano, N. Sulzenauer, J. D. Vieira, D. Vizgan, A. Weiß, and K. E. Whitaker, Nature **618**, 708 (2023).
[9]M. C. McCarthy, K. L. K. Lee, R. A. Loomis, A. M. Burkhardt, C. N. Shingledecker, S. B. Charnley, M. A. Cordiner, E. Herbst, S. Kalenskii, E. R. Willis, C. Xue, A. J. Remijan, and B. A. McGuire, Nat. Astron. **5**, 176 (2020).
[10]D. B. Rap, J. G. M. Schrauwen, A. N. Marimuthu, B. Redlich, and S. Brünken, Nat. Astron. **6**, 1059 (2022).
[11]E. Reizer, B. Viskolcz, and B. Fiser, Chemosphere **291**, 132793 (2022).
[12]A. R. Dixon, D. Khuseynov, and A. Sanov, J. Chem. Phys. **143**, 134306 (2015).
[13]S. Gulania, T.-C. Jagau, A. Sanov, and A. I. Krylov, Phys. Chem. Chem. Phys. **22**, 5002 (2020).
[14]D. B. Rap, A. Simon, K. Steenbakkers, J. G. M. Schrauwen, B. Redlich, and S. Brünken, Faraday Discuss. **245**, 221 (2023).
[15]D. B. Rap, J. G. M. Schrauwen, B. Redlich, and S. Brünken, Phys. Chem. Chem. Phys. **26**, 7296 (2024).
[16]U. Jacovella, J. A. Noble, A. Guliani, C. S. Hansen, A. J. Trevitt, J. Mouzay, I. Couturier-Tamburelli, N. Pietri, and L. Nahon, Astron. Astrophys. **657**, A85 (2022).
[17]A. G. G. M. Tielens, Ann. Rev. Astron. Astrophys. **46**, 289 (2008).
[18]A. G. G. M. Tielens, Rev. Mod. Phys. **85**, 1021 (2013).
[19]E. A. Bergin and M. Tafalla, Ann. Rev. Astron. Astrophys. **45**, 339 (2007).
[20]T. J. Millar, C. Walsh, and T. A. Field, Chem. Rev. **117**, 1765 (2017).
[21]M. Agúndez, J. Cernicharo, M. Guélin, C. Kahane, E. Roueff, J. Kłos, F. J. Aoiz, F. Lique, N. Marcelino, J. R. Goicoechea, M. González García, C. A. Gottlieb, M. C. McCarthy, and P. Thaddeus, Astron. Astrophys. **517**, L2 (2010).
[22]J. Cernicharo, N. Marcelino, J. R. Pardo, M. Agúndez, B. Tercero, P. de Vicente, C. Cabezas, and C. Bermúdez, Astron. Astrophys. **641**, L9 (2020).
[23]J. Cernicharo, J. R. Pardo, C. Cabezas, M. Agúndez, B. Tercero, N. Marcelino, R. Fuentetaja, M. Guélin, and P. de Vicente, Astron. Astrophys. **670**, L19 (2023).
[24]A. J. Remijan, J. M. Hollis, F. J. Lovas, M. A. Cordiner, T. J. Millar, A. J. Markwick-Kemper, and P. R. Jewell, Astrophys. J. **664**, L47 (2007).
[25]J. Cernicharo, M. Guélin, M. Agúndez, K. Kawaguchi, M. McCarthy, and P. Thaddeus, Astron. Astrophys. **467**, L37 (2007).
[26]H. Gupta, C. A. Gottlieb, M. C. McCarthy, and P. Thaddeus, Astrophys. J. **691**, 1494 (2009).
[27]A. Remijan, H. N. Scolati, A. M. Burkhardt, P. B. Changala, S. B. Charnley, I. R. Cooke, M. A. Cordiner, H. Gupta, E. Herbst, K. L. Kelvin Lee, R. A. Loomis, C. N. Shingledecker, M. A. Siebert, C. Xue, M. C. McCarthy, and B. A. McGuire, Astrophys. J. Lett. **944**, L45 (2023).
[28]E. K. Ashworth, S. H. Ashworth, and J. N. Bull, Rev. Sci. Instrum. **95**, 075103 (2024).
[29]G. M. Roberts, J. L. Nixon, J. Lecointre, E. Wrede, and J. R. R. Verlet, Rev. Sci. Instrum. **80**, 053104 (2009).
[30]T. H. Dunning, J. Chem. Phys. **90**, 1007 (1989).
[31]M. J. Frisch, M. Head-Gordon, and J. A. Pople, Chemical Physics Letters **166**, 275 (1990).
[32]R. A. Kendall, T. H. Dunning, and R. J. Harrison, J. Chem. Phys. **96**, 6796 (1992).
[33]J.-D. Chai and M. Head-Gordon, Phys. Chem. Chem. Phys. **10**, 6615 (2008).

[34]M. J. Frisch, G. W. Trucks, H. B. Schlegel, G. E. Scuseria, M. A. Robb, J. R. Cheeseman, G. Scalmani, V. Barone, B. Mennucci, G. A. Petersson, H. Nakatsuji, M. Caricato, X. Li, H. P. Hratchian, A. F. Izmaylov, J. Bloino, G. Zheng, J. L. Sonnenberg, M. Hada, M. Ehara, K. Toyota, R. Fukuda, J. Hasegawa, M. Ishida, T. Nakajima, Y. Honda, O. Kitao, H. Nakai, T. Vreven, J. A. Montgomery, Jr., J. E. Peralta, F. Ogliaro, M. Bearpark, J. J. Heyd, E. Brothers, K. N. Kudin, V. N. Staroverov, R. Kobayashi, J. Normand, K. Raghavachari, A. Rendell, J. C. Burant, S. S. Iyengar, J. Tomasi, M. Cossi, N. Rega, J. M. Millam, M. Klene, J. E. Knox, J. B. Cross, V. Bakken, C. Adamo, J. Jaramillo, R. Gomperts, R. E. Stratmann, O. Yazyev, A. J. Austin, R. Cammi, C. Pomelli, J. W. Ochterski, R. L. Martin, K. Morokuma, V. G. Zakrzewski, G. A. Voth, P. Salvador, J. J. Dannenberg, S. Dapprich, A. D. Daniels, Ö. Farkas, J. B. Foresman, J. V. Ortiz, J. Cioslowski, and D. J. Fox, Gaussian 16 Revision B.01, Gaussian Inc., Wallingford CT 2016.
[35]G. D. Purvis and R. J. Bartlett, J. Chem. Phys. **76**, 1910 (1982).
[36]M. Urban, J. Noga, S. J. Cole, and R. J. Bartlett, J. Chem. Phys. **83**, 4041 (1985).
[37]J. F. Stanton and R. J. Bartlett, J. Chem. Phys. **98**, 7029 (1993).
[38]M. Nooijen and R. J. Bartlett, J. Chem. Phys. **102**, 3629 (1995).
[39]K. B. Bravaya, D. Zuev, E. Epifanovsky, and A. I. Krylov, J. Chem. Phys. **138**, 124106 (2013).
[40]E. Epifanovsky, A. T. B. Gilbert, X. Feng, J. Lee, Y. Mao, N. Mardirossian, P. Pokhilko, A. F. White, M. P. Coons, A. L. Dempwolff, Z. Gan, D. Hait, P. R. Horn, L. D. Jacobson, I. Kaliman, J. Kussmann, A. W. Lange, K. U. Lao, D. S. Levine, J. Liu, S. C. McKenzie, A. F. Morrison, K. D. Nanda, F. Plasser, D. R. Rehn, M. L. Vidal, Z.-Q. You, Y. Zhu, B. Alam, B. J. Albrecht, A. Aldossary, E. Alguire, J. H. Andersen, V. Athavale, D. Barton, K. Begam, A. Behn, N. Bellonzi, Y. A. Bernard, E. J. Berquist, H. G. A. Burton, A. Carreras, K. Carter-Fenk, R. Chakraborty, A. D. Chien, K. D. Closser, V. Cofer-Shabica, S. Dasgupta, M. de Wergifosse, J. Deng, M. Diedenhofen, H. Do, S. Ehlert, P.-T. Fang, S. Fatehi, Q. Feng, T. Friedhoff, J. Gayvert, Q. Ge, G. Gidofalvi, M. Goldey, J. Gomes, C. E. González-Espinoza, S. Gulania, A. O. Gunina, M. W. D. Hanson-Heine, P. H. P. Harbach, A. Hauser, M. F. Herbst, M. Hernández Vera, M. Hodecker, Z. C. Holden, S. Houck, X. Huang, K. Hui, B. C. Huynh, M. Ivanov, Á. Jász, H. Ji, H. Jiang, B. Kaduk, S. Kähler, K. Khistyaev, J. Kim, G. Kis, P. Klunzinger, Z. Koczor-Benda, J. H. Koh, D. Kosenkov, L. Koulias, T. Kowalczyk, C. M. Krauter, K. Kue, A. Kunitsa, T. Kus, I. Ladjánszki, A. Landau, K. V. Lawler, D. Lefrancois, S. Lehtola, R. R. Li, Y.-P. Li, J. Liang, M. Liebenthal, H.-H. Lin, Y.-S. Lin, F. Liu, K.-Y. Liu, M. Loipersberger, A. Luenser, A. Manjanath, P. Manohar, E. Mansoor, S. F. Manzer, S.-P. Mao, A. V. Marenich, T. Markovich, S. Mason, S. A. Maurer, P. F. McLaughlin, M. F. S. J. Menger, J.-M. Mewes, S. A. Mewes, P. Morgante, J. W. Mullinax, K. J. Oosterbaan, G. Paran, A. C. Paul, S. K. Paul, F. Pavošević, Z. Pei, S. Prager, E. I. Proynov, Á. Rák, E. Ramos-Cordoba, B. Rana, A. E. Rask, A. Rettig, R. M. Richard, F. Rob, E. Rossomme, T. Scheele, M. Scheurer, M. Schneider, N. Sergueev, S. M. Sharada, W. Skomorowski, D. W. Small, C. J. Stein, Y.-C. Su, E. J. Sundstrom, Z. Tao, J. Thirman, G. J. Tornai, T. Tsuchimochi, N. M. Tubman, S. P. Veccham, O. Vydrov, J. Wenzel, J. Witte, A. Yamada, K. Yao, S. Yeganeh, S. R. Yost, A. Zech, I. Y. Zhang, X. Zhang, Y. Zhang, D. Zuev, A. Aspuru-Guzik, A. T. Bell, N. A. Besley, K. B. Bravaya, B. R. Brooks, D. Casanova, J.-D. Chai, S. Coriani, C. J. Cramer, G. Cserey, A. E. DePrince III, R. A. DiStasio Jr., A. Dreuw, B. D. Dunietz, T. R. Furlani, W. A. Goddard III, S. Hammes-Schiffer, T. Head-Gordon, W. J. Hehre, C.-P. Hsu, T.-C. Jagau, Y. Jung, A. Klamt, J. Kong, D. S. Lambrecht, W. Liang, N. J. Mayhall, C. W. McCurdy, J. B. Neaton, C. Ochsenfeld, J. A. Parkhill, R. Peverati, V. A. Rassolov, Y. Shao, L. V. Slipchenko, T. Stauch, R. P. Steele, J. E. Subotnik, A. J. W. Thom, A. Tkatchenko, D. G. Truhlar, T. Van Voorhis, T. A. Wesolowski, K. B. Whaley, H. L. Woodcock III, P. M. Zimmerman, S. Faraji, P. M. W. Gill, M. Head-Gordon, J. M. Herbert, and A. I. Krylov, J. Chem. Phys. **155**, 084801 (2021).
[41]R. N. Zare, Mol. Photochem. **4**, 1 (1972).
[42]S. Gozem and A. I. Krylov, WIREs Comput. Mol. Sci. **12**, e1546 (2021).
[43]V. Barone, J. Bloino, M. Biczysko, and F. Santoro, J. Chem. Theory Comput. **5**, 540 (2009).
[44]E. P. Wigner, Phys. Rev. **73**, 1002 (1948).
[45]R. A. Firth, T. L. Dimino, and W. K. Gichuhi, J. Phys. Chem. A **126**, 4781 (2022).
[46]E. Fermi and E. Teller, Phys. Rev. **72**, 399 (1947).
[47]W. R. Garrett, Phys. Rev. A **3**, 961 (1971).
[48]C.-H. Qian, G.-Z. Zhu, and L.-S. Wang, J. Phys. Chem. Lett. **10**, 6472 (2019).
[49]R. F. Gunion, M. K. Gilles, M. L. Polak, and W. Lineberger, Int. J. Mass Spectrom. Ion Proc. **117**, 601 (1992).
[50]M. L. Theis, A. Candian, A. G. G. M. Tielens, T. J. Lee, and R. C. Fortenberry, Phys. Chem. Chem. Phys. **17**, 14761 (2015).
[51]J. N. Bull, C. W. West, and J. R. R. Verlet, Phys. Chem. Chem. Phys. **17**, 16125 (2015).
[52]E. K. Ashworth, C. S. Anstöter, J. R. R. Verlet, and J. N. Bull, Phys. Chem. Chem. Phys. **23**, 5817 (2021).
[53]J. N. Bull, C. W. West, and J. R. R. Verlet, Chem. Sci. **6**, 1578 (2015).
[54]C. E. Klots, Chem. Phys. Lett. **186**, 73 (1991).
[55]J. N. Bull, C. W. West, and J. R. R. Verlet, Phys. Chem. Chem. Phys. **17**, 32464 (2015).
[56]P. J. Sarre, Monthly Notices of the Royal Astronomical Society **313**, L14 (2000).
[57]M. Khamesian, N. Douguet, S. Fonseca dos Santos, O. Dulieu, M. Raoult, W. J. Brigg, and V. Kokoouline, Phys. Rev. Lett. **117**, 123001 (2016).
[58]A. Léger, P. Boissel, and L. d'Hendecourt, Phys. Rev. Lett. **60**, 921 (1988).
[59]R. Chacko, S. Banhatti, M. Nrisimhamurty, J. K. Yadav, A. K. Gupta, and G. Aravind, Astrophys. J. **905**, 90 (2020).
[60]M. Agúndez, N. Marcelino, B. Tercero, I. Jiménez-Serra, and J. Cernicharo, Astron. Astrophys. **677**, A106 (2023).
[61]M. Lara-Moreno, T. Stoecklin, and P. Halvick, ACS Earth Space Chem. **3**, 1556 (2019).
[62]R. D. Thomas, H. T. Schmidt, G. Andler, M. Björkhage, M. Blom, L. Brännholm, E. Bäckström, H. Danared, S. Das, N. Haag, P. Halldén, F. Hellberg, A. I. S. Holm, H. A. B. Johansson, A. Källberg, G. Källersjö, M. Larsson, S. Leontein, L. Liljeby, P. Löfgren, B. Malm, S. Mannervik, M. Masuda, D. Misra, A. Orbán, A. Paál, P. Reinhed, K.-G. Rensfelt, S. Rosén, K. Schmidt, F. Seitz, A. Simonsson, J. Weimer, H. Zettergren, and H. Cederquist, Rev. Sci. Instrum. **82**, 065112 (2011).
[63]J. N. Bull, M. S. Scholz, E. Carrascosa, M. K. Kristiansson, G. Eklund, N. Punnakayathil, N. de Ruette, H. Zettergren, H. T. Schmidt, H. Cederquist, and M. H. Stockett, J. Chem. Phys. **151**, 114304 (2019).
[64]M. H. Stockett, J. N. Bull, J. T. Buntine, E. Carrascosa, E. K. Anderson, M. Gatchell, M. Kaminska, R. F. Nascimento, H. Cederquist, H. T. Schmidt, and H. Zettergren, Eur. Phys. J. D **74**, 150 (2020).
[65]M. H. Stockett, J. N. Bull, H. Cederquist, S. Indrajith, M. Ji, J. E. Navarro Navarrete, H. T. Schmidt, H. Zettergren, and B. Zhu, Nat. Commun. **14**, 395 (2023).
[66]J. W. L. Lee, M. H. Stockett, E. K. Ashworth, J. E. Navarro Navarrete, E. Gougoula, D. Garg, M. Ji, B. Zhu, S. Indrajith, H. Zettergren, H. T. Schmidt, and J. N. Bull, J. Chem. Phys. **158**, 174305 (2023).
[67]M. Saito, H. Kubota, K. Yamasa, K. Suzuki, T. Majima, and H. Tsuchida, Phys. Rev. A **102**, 012820 (2020).
[68]B. T. Draine, Astrophys. J. Supp. Ser. **36**, 595 (1978).
[69]T. Pino, M. Tulej, F. Güthe, M. Pachkov, and J. P. Maier, J. Chem. Phys. **116**, 6126 (2002).

[70]T. A. Yen, E. Garand, A. T. Shreve, and D. M. Neumark, J. Phys. Chem. A **114**, 3215 (2009).
[71]T. R. Taylor, C. Xu, and D. M. Neumark, J. Chem. Phys. **108**, 10018 (1998).
[72]W. Skomorowski, S. Gulania, and A. I. Krylov, Phys. Chem. Chem. Phys. **20**, 4805 (2018).
[73]S. Klaiman, E. V. Gromov, and L. S. Cederbaum, J. Phys. Chem. Lett. **4**, 3319 (2013).
[74]B. Concina and C. Bordas, J. Phys. Chem. A **126**, 7442 (2022).